HEPATOLOGY

HEPATOLOGY, VOL. 65, NO. 5, 2017

Human Macrophage Ferroportin Biology and the Basis for the Ferroportin Disease

Manuela Sabelli,[1] Giuliana Montosi,[1] Cinzia Garuti,[1] Angela Caleffi,[1] Stefania Oliveto,[2] Stefano Biffo,[2,3] and Antonello Pietrangelo[1]

Ferroportin (FPN1) is the sole iron exporter in mammals, but its cell-specific function and regulation are still elusive. This study examined FPN1 expression in human macrophages, the cells that are primarily responsible on a daily basis for plasma iron turnover and are central in the pathogenesis of ferroportin disease (FD), the disease attributed to lack-of-function FPN1 mutations. We characterized FPN1 protein expression and traffic by confocal microscopy, western blotting, gel filtration, and immunoprecipitation studies in macrophages from control blood donors (donor) and patients with either FPN1 p.A77D, p.G80S, and p.Val162del lack-of-function or p.A69T gain-of-function mutations. We found that in normal macrophages, FPN1 cycles in the early endocytic compartment does not multimerize and is promptly degraded by hepcidin (Hepc), its physiological inhibitor, within 3-6 hours. In FD macrophages, endogenous FPN1 showed a similar localization, except for greater accumulation in lysosomes. However, in contrast with previous studies using overexpressed mutant protein in cell lines, FPN1 could still reach the cell surface and be normally internalized and degraded upon exposure to Hepc. However, when FD macrophages were exposed to large amounts of heme iron, in contrast to donor and p.A69T macrophages, FPN1 could no longer reach the cell surface, leading to intracellular iron retention. *Conclusion*: FPN1 cycles as a monomer within the endocytic/plasma membrane compartment and responds to its physiological inhibitor, Hepc, in both control and FD cells. However, in FD, FPN1 fails to reach the cell surface when cells undergo high iron turnover. Our findings provide a basis for the FD characterized by a preserved iron transfer in the enterocytes (i.e., cells with low iron turnover) and iron retention in cells exposed to high iron flux, such as liver and spleen macrophages. (HEPATOLOGY 2017;65:1512-1525)

Ferroportin (FPN1), the only iron exporter identified in mammals, is involved in iron transfer from the external milieu and from internal sites of iron storage and recycling into the bloodstream.[1] At the systemic level, FPN1 is mainly controlled posttranslationally by hepcidin (Hepc), which binds to FPN1 at the cell surface and causes its degradation.[2]

The predicted molecular mass of purified human FPN1 is approximately 69 ± 6.2 kDa.[3] Yet, in mouse tissues, different FPN1 molecular weight (MW) forms have been detected in liver, duodenum, and spleen.[4] FPN1 topology and membrane organization has also been addressed with controversial results concerning localization of the N- and C-termini and number of transmembrane segments.[3,5-13]

Abbreviations: aa, amino acid; BME, ß-mercaptoethanol; BPB, bromophenol blue; DAPI, 4',6-diamidino-2-phenylindole; Dx, dexamethasone phosphate; EDTA, ethylenediaminetetraacetic acid; EEA-1, early endosome antigen 1; eEF1A, eukaryotic elongation factor 1A; eIF6, eukaryotic translation initiation factor 6; Endo H, endoglycosidase H; FD, ferroportin disease; FPN1, ferroportin; Hb, hemoglobin; Hepc, hepcidin; IAA, iodoacetamide; IP, Immunoprecipitation; LAMP-1, lysosomal-associated membrane protein 1; MDCK, Madin-Darby canine kidney cells; MW, molecular weight; Na,K-ATPase, sodium-potassium pump; PBMCs, peripheral blood mononuclear cells; PBS, phosphate-buffered saline; PNGase F, peptide N-glycosidase F; RT, room temperature; SDS, sodium dodecyl sulfate; SDS-PAGE, SDS/polyacrylamide gel electrophoresis; TE, total protein extract; TEP, trypsin-EDTA-PBS; TfR1, transferrin receptor 1; WB, western blotting; WT, wild type.

Received March 10, 2016; accepted December 15, 2016.

Additional Supporting Information may be found at onlinelibrary.wiley.com/doi/10.1002/hep.29007/suppinfo.

Supported by PRIN 2010-201 no. 2010REYFZH_005, Strategic research Program Region Emilia Romagna-University 2010-12, Programma di Ricerca Regione-Università 2010-2012, and Telethon Contract no. GGP14285 2014-2017 (to A.P.).

View this article online at wileyonlinelibrary.com.

DOI 10.1002/hep.29007

Potential conflict of interest: Nothing to report.

Dissecting the basis of the human disease attributed to lack of FPN1, the so-called ferroportin disease (FD),[14] would be informative also for understanding protein biology and function. FD is an autosomal-dominant disorder attributed to lack-of-function mutations of FPN1 and is characterized by marked iron accumulation in tissue macrophages, preserved intestinal iron transfer, and subclinical anemia.[15,16] Unusual gain-of-function mutations of FPN1 (such as N144H, C326Y, and C326S)[17-19] prevent Hepc binding and/or FPN1 internalization, so that, although hepcidin is produced normally, FPN1 is resistant to its inhibitory activity and persistently exports iron toward the bloodstream, ultimately resulting in syndrome identical to hemochromatosis but distinct from FD.

A number of *in vitro* studies, mostly using overexpressed exogenous wild-type (WT) and mutant FPN1 in a variety of cell lines, have investigated FPN1 biology and function and have provided valuable information on the effect of different FPN1 mutants on protein traffic and iron transfer capability.[3,5-7,9,12,20-26]

In this context, it has been actively debated whether FPN1 haploinsufficiency would explain FD or whether the disease results from a dominant-negative effect. It has been argued that if haploinsufficiency was the explanation for FD, then nonsense mutations should also result in the disorder; however, so far, the vast majority of reported mutations in FD are missense mutations.[27] Additionally, a targeted gene deletion in the murine Fpn1 gene has little effect in heterozygous animals,[28] whereas the flatiron (ffe) mouse, with a missense mutation in Fpn1 that affects its localization and iron export activity when overexpressed *in vitro*, presents a phenotype similar to human patients.[8] Finally, exogenous tagged FPN1 *in vitro* forms multimers and mutant Fpn1 prevents cell membrane localization of WT Fpn1.[8,21,29] However, other studies from different groups reached opposite conclusions, showing that Fpn1 is a monomer in cultured cells[3,30,31] and *in vivo* in mice.[32]

Given that it is formally possible that FD in mice cannot recapitulate the human disease and that artificial overexpression of FPN1 in cultured cells may not reproduce the physiological state, we directly investigated FPN1 expression in human macrophages from control blood donors and from patients with FD.

Patients and Methods

PATIENTS

The study included members of four different pedigrees carrying the p.A77D, p.G80S, p.Val162del, and p.A69T FPN1 mutations (Fig. 1). Blood was also collected from age- and sex-matched blood donors with normal iron status. The study was approved by the ethics committee at the University of Modena (Modena, Italy) and Reggio Emilia.

PROCESSING OF BIOPSY SPECIMENS

Five-micrometer liver biopsy sections were immersed in a 4% solution of paraformaldehyde in buffer/L 0.1 mol of phosphate-buffered saline (PBS; pH 7.4), embedded in paraffin, and stained with Perls' Prussian blue for the presence of iron.

CELL CULTURE

Peripheral Blood Mononuclear Cells Isolation and Culture

Monocytes were obtained by gradient centrifugation of peripheral blood mononuclear cells (PBMCs) and cultured as described.[33] At day 3, 25 ng/mL of granulocyte colony-stimulating factor (Invitrogen Corporation, Carlsbad, CA, USA) were added, and macrophages were selected by adhesion. Medium and all reagents were endotoxin free.

ARTICLE INFORMATION:

From the [1]Division of Internal Medicine 2 and Center for Hemochromatosis, University Hospital of Modena, Modena, Italy; [2]INGM, 'Romeo ed Enrica Invernizzi', Milano, Italy; and [3]Department of Biosciences, University of Milan, Milan, Italy.

ADDRESS CORRESPONDENCE AND REPRINT REQUESTS TO:

Antonello Pietrangelo, M.D., Ph.D.
Professor of Medicine
Director, Division of Internal Medicine 2 and
Center for Hemochromatosis
University Hospital of Modena Via del Pozzo 71
41100 Modena, Italy
E-mail: antonello.pietrangelo@unimore.it
Tel. + 390594224356

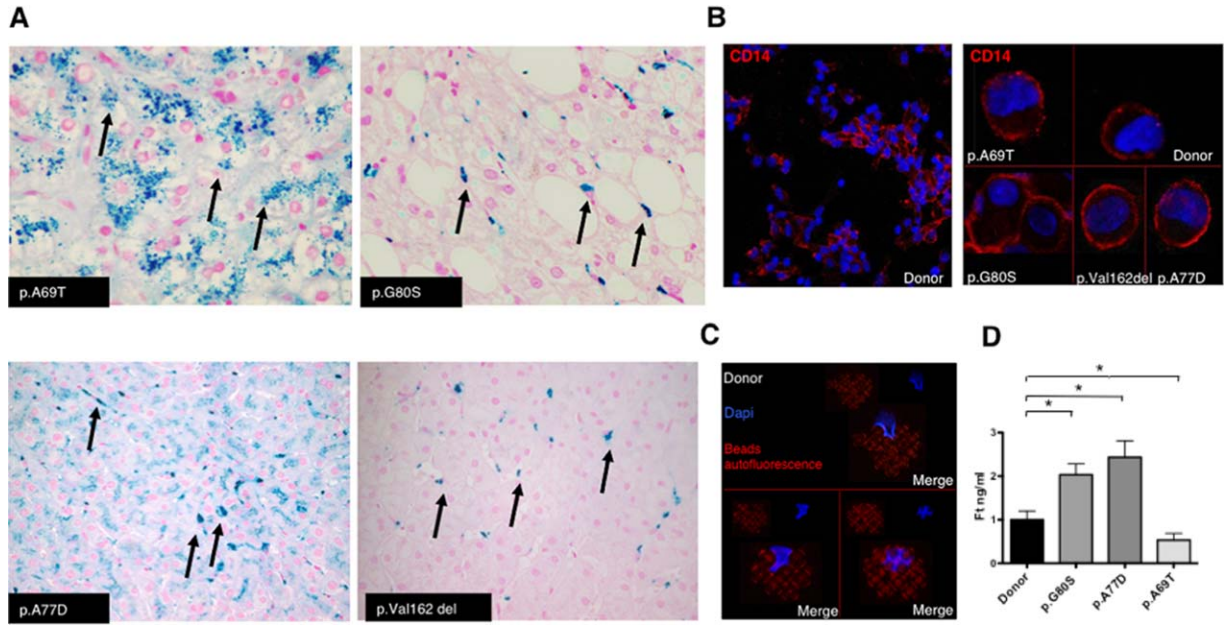

FIG. 1. Liver and macrophage phenotype of FD patients. (A) Liver biopsy sections from patients with FD investigated in this study stained with Perls' Prussian blue for iron. Pictures show the classic iron-laden phenotype of Kupffer cells (arrows) in p.A77D, p.G80S, and pVal162del FD patients. On the contrary, microphotograph from a patient carrying the p.A69T FPN1 mutation shows iron accumulation in hepatocytes, but not in Kupffer cells. Donor and disease PBMC-derived macrophages (B) express after 7 days the CD14 macrophage-specific marker and (C) retain normal phagocytic activity when incubated in the presence of autofluorescent beads (see Patients and Methods). (D) Ferritin content of representative macrophage preparations. The amount of intracellular ferritin is doubled in macrophages from lack-of-function FD patients and halved in macrophages from patients carrying the Hepc-resistant p.A69T mutation. Ferritin values are mean ± SEM of three different cell preparations from a representative patient as compared to cell preparations from a blood donor. $^{*}P < 0.05$.

Macrophage lineage characterization was based on morphological study and expression of the monocytes-macrophages lineage marker, CD14 (see below).

To block dynamin-dependent endocytosis,[34] *in vitro* differentiated macrophages were treated with 40 and 400 μM of dynasore (Enzo Life Sciences, Lausen, Switzerland) for 30 minutes and processed for immunoflurescence.

Cells were also treated for 1-24 hours with 700 nM of Hepc (Peptide Institute, Minoh-shi Osaka, Japan) and subjected to immunofluorescence.

In specific experiments, cells were preincubated for 18 hours with 0.25 μM of dexamethasone phosphate (Dx; Sigma-Aldrich, St. Louis, MO, USA), a known stimulator of CD163 expression and hemoglobin (Hb) uptake by macrophages,[35] and then incubated for 6 hours with 20 μg/mL of bovine Hb (Sigma-Aldrich). Donor macrophages were also treated with aged red blood cells as reported.[36] Cells were harvested and processed for immunofluorescence.

Cellular ferritin content and iron in the medium were assayed after overnight incubation as specified below.

FPN-1-Expressing Cell Lines

Full-length FPN1 complementary DNA was generated by RT-PCR amplification of human fibroblast RNA. DNA gene sequencing by Sanger confirmed that the donor human fibroblast *SCL40A1* gene was WT. The FPN1 coding region was sequenced and subcloned into the pcDNA3.1/Hygro expression vector (Invitrogen, Groningen, The Netherlands), in order to obtain FPN1 untagged or tagged at the C-terminal with V5 epitope. The pA77D FPN1 was obtained by mutagenesis using the QuickChange Site-Directed Mutagenesis kit (Stratagene, Milan, Italy). Madin-Darby canine kidney cells (MDCK) cells stably expressing WT, pA77D FPN1, and FPN1-V5 were obtained by transfecting MDCK cells with the Transfection Reagent Selector Kit Effectane (Qiagen,

Milan, Italy), according to the manufacturer's instructions.

Differentiation of THP-1 Cell Line

In order to differentiate the human leukemia cell line, THP-1, to macrophages, cells were incubated in RPMI 1640 medium containing phorbol 12-myristate 13-acetate at 5 ng/mL for 48 hours, as reported by Park et al.[37]

IMMUNOPRECIPITATION AND WESTERN BLOTTING ANALYSIS

Whole-cell lysates from PMBC-derived macrophages, THP1 (human leukemia cell line), MDCK cells, and MDCK stably transfected with WT, pA77D human FPN1, and human FPN1-V5 were subjected to western blotting (WB) analysis using the ECL Advance WB Detection Kit (GE Healthcare Life Sciences, Milan, Italy) according to the manufacturer's instructions. Total proteins were extracted with trypsin-EDTA-PBS (TEP) lysis buffer (150 mm of NaCl, 10 mM of Tris [pH = 8], 10 mM of ethylenediaminetetraacetic acid [EDTA], and 1% Triton X-100) supplemented with 1:100 protease inhibitor cocktail (Sigma-Aldrich) for standard WB, or, in specific experiments, supplemented with 50 mM of iodoacetamide (IAA; Sigma-Aldrich). After centrifugation at 13,000*g* at 4 °C for 15 minutes, the supernatant was collected and protein concentration assayed by the Bradford method. In specific experiments, samples were heated 10 minutes at 100 °C, in loading buffer with 100 mM of 1,4-dithiotheitol or 2.5% β-mercaptoethanol (BME). The antibodies used in WB analysis were as follows: rabbit anti-FPN1 that recognizes a 19-amino-acid (aa) epitope on FPN1 C-terminal (1:10,000; Alpha Diagnostic International, San Antonio, TX), or rabbit anti-FPN1 antibody (1:2,000) that recognizes an epitope 223-303 aa localized on an intracellular loop beetwen VI and VII transmembrane domain, kindly provided by D.J. Haile,[38] followed by horseradish peroxidase–conjugated swine anti-rabbit antibody (1:10,000; Dako Cytomation, Glostrup, Denmark), as secondary antibody.

Immunoprecipitation (IP) studies were performed as described.[32] In brief, FPN1 in cleared lysates was immunoprecipitated by adding 5 mg/mg of rabbit anti-FPN1 antibody for 2 hours at 4 °C, followed by overnight incubation with 50 mL/mg of equilibrated protein A-Sepharose 4B/protein G-Sepharose resin (Sigma-Aldrich). The beads were extensively washed with TEP buffer and protein solubilized in protein loading buffer (sodium dodecyl sulfate [SDS] 2%, glycerol 10%, BME 2.5%, 62.5 mM of Tris-HCl [pH = 6.8], and bromophenol blue [BPB] 0.01%) for 30 minutes, at room temperature (RT). Total protein extracts (25 μg) and immunoprecipitates were run on 10% SDS-PAGE (polyacrylamide gel electrophoresis) and blotted onto nitrocellulose membrane at 150 mAmp overnight, at RT.

GEL FILTRATION

Macrophage extracts in TEP lysis buffer were loaded on a Superose 12 10/300 GL column (GE Healthcare Life Sciences). Chromatography was run at a flow rate of 1 mL/min, and fractions of 1.5 mL were eluted. After trichloroacetic acid precipitation, each fraction was directly loaded on SDS-PAGE and probed with rabbit anti-Fpn1 or rabbit anti-eEF1A (eukaryotic elongation factor 1A; Cell Signaling Technology) or mouse anti-eIF6 (eukaryotic translation initiation factor 6)[39] antibodies.

MEMBRANE PROTEIN BIOTINYLATION

Macrophages and human liver hepatocellular carcinoma cell line (HepG2) were incubated in ice with sulfo-NHS-Biotin (Pierce Protein Biology–Thermo Fisher Scientific Inc, Rockford, IL) at a concentration of 2 mM diluted in PBS for 30 minutes; afterward, the labeling reaction was blocked with cell-culture medium and cells washed with PBS. Total proteins were extracted with TEP buffer or buffer 2 (150 mm of NaCl, 100 mM of phosphate, 1% Triton-X, and 10 mM of EDTA) supplemented with a protease inhibitor cocktail (1:100; Sigma-Aldrich). Total protein extracts were then incubated for 18 hours at 4 °C with agarose beads conjugated to streptavidin (Pierce Protein Biology–Thermo Fisher Scientific), and, after repeated washing with lysis buffer, samples were eluted in protein loading buffer (2% SDS, 62.5 mM of Tris base [pH = 6.8], 10% glycerol, 2.5% 2-mercaptoethanol, and BPB 0.01%), under went shaking for 30 minutes at RT and for an additional 30 minutes at 37 °C. Total protein extracts (25 μg) and eluted samples were subjected to SDS-PAGE followed by WB analysis, as described.

IMMUNOFLUORESCENCE

Cells were washed with PBS and fixed in cold (t = –20 °C) 100% methanol for 10 minutes at RT and first incubated in blocking solution (4% goat serum in PBS) for 1 hour at RT and then with the primary and secondary antibody diluted in blocking solution or PBS for one additional hour. To detect Hepc expression, incubation with the primary antibody was performed for 18 hours at 4 °C. The primary antibodies used were: mouse antihuman CD14 (1:20; Chemicon International, Temecula, CA); mouse anti–sodium-potassium pump (Na,K-ATPase [plasma membrane marker]; 1:500, Abcam, Cambridge, UK); rabbit anticalnexin (1:200 [endoplasmic reticulum marker]; Sigma-Aldrich); rabbit anti-golgin-97 (1:100 [Golgi marker]; Molecular Probes, Leiden, The Netherlands)(Golgi marker); rabbit anti–early endosome antigen 1 (EEA-1; 1:200; Abcam, Cambridge, UK), as an early endosomes marker; rat anti–lysosomal-associated membrane protein 1 (LAMP-1 [lysosome marker]; 1:50; Fitzgerald Industries International, Concord, MA); rabbit anti-FPN1 (1:50 PBS; Alpha Diagnostic International, San Antonio, TX, USA); rabbit anti–human transferrin receptor 1 (TfR1; 1:50; Santa Cruz Biotechnology, Santa Cruz, CA); and rabbit anti-Hepc (1:50 PBS; Alpha Diagnostic International). Secondary antibodies were: goat antimouse Alexa 594 coniugated (1:400; Sigma-Aldrich); goat antirabbit Alexa 594 coniugated (1:300; Sigma-Aldrich); rabbit antirat (1:50; Dako Cytomation, Glostrup, Denmark); and goat antirabbit Alexa 488 coniugated (1:200; Sigma-Aldrich). Afterward, cells were incubated in 4',6-diamidino-2-phenylindole (DAPI) 2 ng/μL of PBS for 5 minutes at RT to highlight nuclei and analyzed by a Leica confocal microscopy.

FERRITIN AND IRON MEASUREMENTS

Total proteins were extracted from macrophages with lysis buffer TEP (150 mm of NaCl, 10 mM of Tris [pH = 8], 0.5% Triton-X, and 1 mM of EDTA) supplemented with protease inhibitor cocktail (1:100; Sigma-Aldrich). After centrifugation at 13,000*g* at 4 °C for 15 minutes, the supernatant was collected and protein assayed by the Bradford method. Ferritin was measured by enhanced particle immunoturbidimetric assay (Roche Diagnostics, Indianapolis, IN, USA), and the values obtained were normalized to the protein content.

For iron assay, cell media were collected and cell debris were removed by centrifugation. After lyophilization, samples were digested in ultrapure 65% nitric acid for 18 hours at RT and for an additional 2 hours at 120 °C in the presence of hydrogen peroxide (Sigma-Aldrich) to improve mineralization. Finally, samples were diluted with ultrapure water and read in triplicate using quadrupole inductively coupled plasma mass spectrometry (Thermo Scientific, Waltham, MA, USA).

STATISTICAL ANALYSIS

All analyses were conducted using Prism 5 for mac OS X (version 5.0a) software. All comparisons were made by using nonparametric statistical tests (GraphPad Software Inc., La Jolla, CA, USA).

Results

PBMCs were obtained from blood donors and patients diagnosed with an FD based on clinical, genetic, and histopathological evaluation. As expected, liver histology showed a predominant iron-laden Kupffer cell pattern typical of the FD, in patients carrying the p.A77D, p.G80S, and p.Val162del FPN1 mutations, whereas patients carrying the Hepc-resistant p.A69T FPN1 mutation showed iron-spared Kupffer cells and selective iron accumulation in hepatocytes (Fig. 1A). As to the PBMC studies, we confirmed that after 7 days of culture, adherent cells expressed the macrophage lineage CD14 marker (Fig. 1B), preserved a phagocytic activity (Fig. 1C), and retained in culture the iron phenotype of the original patient, showing increased ferritin iron content in FD macrophages and lower in p.A69T macrophages (Fig. 1D). Individual patients' macrophages were studied in different occasions, and each time we also ran the experiment in a matched donor.

CHARACTERIZATION OF FPN1 EXPRESSION IN HUMAN MACROPHAGES AND CELL LINES

In preliminary experiments, we verified whether the anti-FPN1 antibody could detect both human WT and mutant FPN1. To this purpose, MCDK cells, in which FPN1 protein is normally undetectable and have been previously used to validate anti-FPN1 antibodies,[28] were stably transfected with WT or A77D mutant human FPN1. In both cases, a predominant FPN1 ~100-kDa MW form was identified by WB (Fig. 2A, lanes 2 and 3), as well as a ~65-kDa band

comigrating with mouse spleen FPN1 (Fig. 2A, lanes 2, 3, and 5). A similar ~100-kDa MW form was also found in a human monocytic cell line (THP-1; Fig. 2A, lane 4, arrow), whereas in mouse spleen, a ~65-kDa MW band was identified by the same antibody (Fig. 2A, lane 5, arrow). In total protein extracts (TE) of donor macrophages, in addition to the ~100-kDa form (Fig. 2B, lane 3a), ~55-kDa MW and 210-kDa MW bands were detected (Fig. 2B). All these forms, that is, the ~55-kDa MW, ~100-kDa MW, and 210-kDa MW, may represent aggregates of unfolded ~55-kDa monomers that multimerize through their multiple transmembrane hydrophobic domains.[40,41] Importantly, heating in the presence of the reducing agent, IAA, that reduces artifactual postlysis aggregation led to the disappearance of the 210-kDa MW band, the reduction of the ~55-kDa and 100-kDa bands, and the enrichment in the expected ~65-kDa band (Fig. 2B, lane 2b). Next, we performed gel filtration assays on macrophage extracts (Fig. 2C). The expected 65-kDa band (b) partitioned in fraction 5, consistent with a monomeric form, and in fraction 2, consistent with its presence in a larger complex, ≥250 kDa (e.g., solubilized microsomal membranes). The 100-kDa form (a) enriched in fraction 3. The ~55-kDa band (c) partitioned throughout the gel filtration (Fig. 2C), suggesting that it is unfolded or prone to form artifactual intermediates. eEF1A, used as a 50-kDa control, partitioned in fraction 2 containing ribosomes, and in monomeric form in fraction 5 as expected, with trailing attributed to solubilization conditions. eIF6, a 27-kDa protein that may form dimers and trimers in native filtration, here used as a 27- to 81-kDa marker, partitioned in fractions 4 and 5. These data, taken together, suggest that FPN1 is a multiple-pass transmembrane protein that may aggregate *ex vivo*, but it exists, *in vivo*, in two stable forms, a monomeric one, and one associated with high-MW structures/microsomal membranes.

Specificity of the anti-FPN1 antibody was proved by the peptide competition experiments showing the disappearance of the macrophage- and spleen-specific bands following preabsorption of the anti-FPN1 antibody with a control peptide (Supporting Figs. S1A and S2B) and by the identification of the same WB pattern using two different anti-FPN1 antibodies (Supporting Fig. S2A). In addition, experiments in HepG2 cells transfected with FPN1-specific small interfering RNA showed a decrease of the relevant FPN1 bands as detected by WB (Supporting Fig. S1C). When analyzing FPN1 expression in TE extracts from diseased macrophages by WB, we found the same FPN1 expression pattern as in donor macrophages (Fig. 2D). All FPN1 electrophoretic forms were also detected in biotinylated human macrophage membrane protein preparations (Fig. 2E).

To investigate whether FPN1 was glycosylated, we subjected macrophage protein extracts to enzymatic digestion with peptide N-glycosidase F (PGNaseF) and endoglycosidase H (EndoH). Supporting Fig. S3 shows that whereas mouse spleen FPN1 was fully digested by PNGase F (Supporting Fig. S3A, lane 1 and 2), as reported,[4] HepG2-FPN1was only partly digested (Supporting Fig. S3B, lane 3), whereas human donor and FD macrophages as well as THP-1-FPN1 were resistant to enzymatic digestion (Supporting Fig. S3C,D).

DISTINCT SUBCELLULAR LOCALIZATION OF FPN1 IN MACROPHAGES FROM BLOOD DONORS AND FD PATIENTS

In donor macrophages, using an immunofluorescence colocalization approach, we found that FPN1 was mostly localized in the early endosome compartment and barely detectable at the plasma membrane (Fig. 3A, Donor, merge panel). Interestingly, also in FD macrophages (from patients with p.A77D, p.G80S, and p.Val162del), the immunofluorescence pattern showed a similar distribution except for a higher amount of FPN1 stain in the lysosomal compartment (Fig. 3A). This was not the case for p.A69T macrophages, which presented an FPN1 immunofluorescence pattern identical to that of donor macrophages.

Using TfR1, a marker for the early/recycling endosome compartment, we found that FPN1 colocalizes with TfR1, indicating that FPN1 traffics within the early/recycling endosome compartment (Fig. 3B). In fact, treatment of macrophages with dynasore, an inhibitor of dynamin-dependent endocytosis, led to a marked increase of plasma membrane localization of both TfR1 and FPN1, with almost no residual signal in the cytoplasm, in both normal and diseased macrophages (Fig. 3C).

RESPONSE TO Hepc-INDUCED FPN1 DEGRADATION IN NORMAL AND DISEASED MACROPHAGES

Exposure of donor macrophages to Hepc, the physiological inhibitor of FPN1, led to a progressive FPN1 degradation starting at 3 hours and peaking at 6 hours, with a full protein re-expression at 24 hours

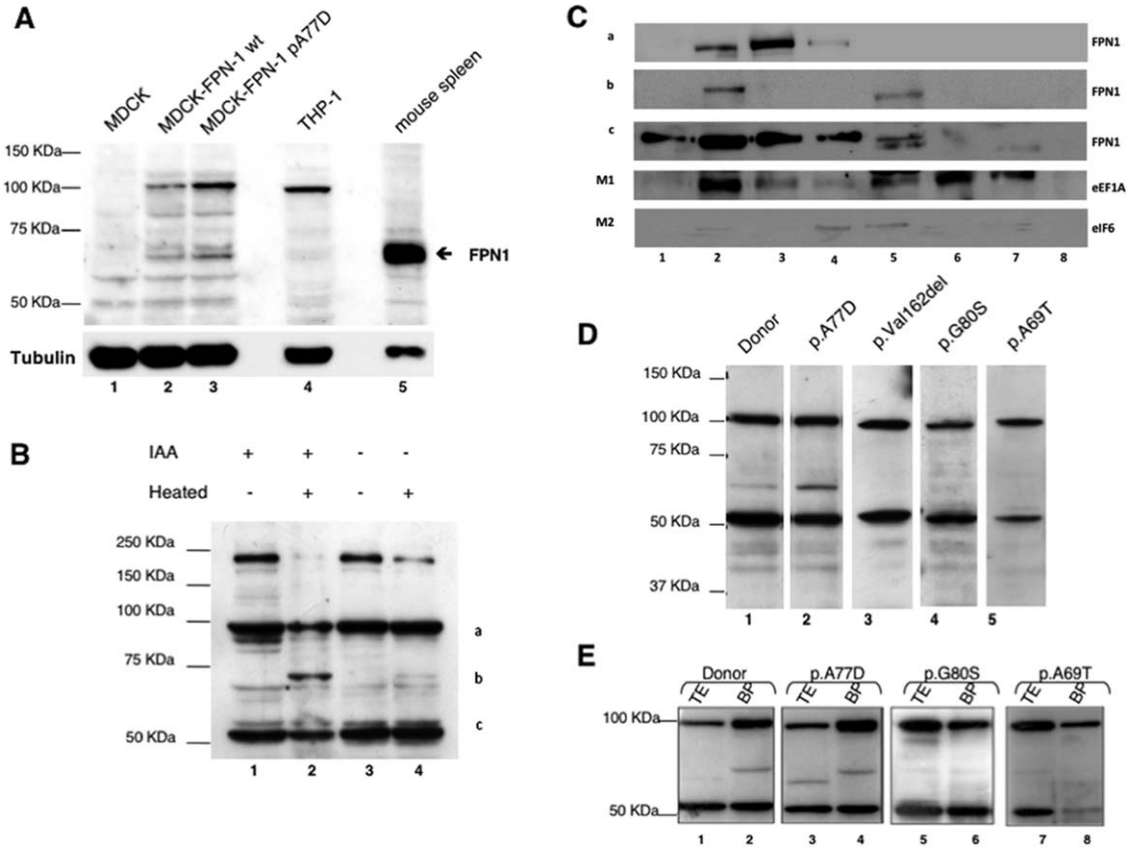

FIG. 2. Characterization of human FPN1. (A) WB analysis for FPN1 in whole-cell lysates from MDCK cells, MDCK stably transfected with WT (MDCK-FPN1) or pA77D (MDCK-FPN1 pA77D) human FPN1 and THP1 cells (THP1) showing different MW forms of FPN1 (arrows; see text for details). (B) WB analysis of whole-cell lysates of healthy donor macrophages extracted with or without IAA, a compound that avoids oxidation of reduced disulfide bonds, and subjected or not to heating (see Patients and Methods for details). The 100- and ~55-kDa MW forms of FPN1 were unaffected by IAA and/or heating (lanes 1 and 4), whereas a 210-kDa MW form originated a 65-kDa MW form after IAA/heating (lane 2; see text for details). a, b, and c on the right indicate the different electrophoretic forms of FPN1 (see panel C and text for discussion). (C) Gel filtration chromatography fractions from macrophage extracts loaded on SDS-PAGE and probed with rabbit anti-FPN1 or rabbit anti-eEF1A or mouse anti-eIF6 antibodies (see Materials and Methods for details). FPN1 protein migration is consistent with a monomeric form and with association with high-MW structures (see text for details). eEF1A and eIF6 were used as control marker (M1 and M2). eEF1A is 50 kDa; trailing to lower fractions is attributed to detergents. eIF6 is 27 kDa MW that, in these conditions, behaves as monomer-dimer-trimer (27-81 kDa). a, b, and c on the left indicate the different electrophoretic forms of FPN1 (see panel B and text for discussion). (D) WB analysis of FPN1 in whole-cell lysates from donor and patient (p.A77D, p.Val162del, p.G80S, and p.A69T) macrophages showing consistent identification of the two main 100- and 55-KDa MW FPN1 forms (lanes 1 through 5). (E) WB analysis identifies the same two main ~100-kDa and ~50-kDa MW forms of FPN1 in plasma membrane proteins from both donor and patients' macrophages after biotinylation and purification with streptavidin agarose beads. Abbreviation: BP, biotinylated proteins.

(Fig. 4A). As expected, in p.A69T mutant cells, FPN1 signal was still present after 3-6 hours Hepc exposure, suggesting that FPN1 was indeed resistant to Hepc inhibition. Apparently, FPN1 stain persisted after 3-6 hours of exposure to hepcidin in all FD macrophages and showed some decrease only in G80S macrophages at 6 hours of exposure (see Discussion). Hepc/FPN1 colocalization studies indicated that upon Hepc exposure in donor macrophages, FPN1 is first recruited to the plasma membrane (Fig. 4B, 1 hour, donor panel), internalized with Hepc, and finally degraded (Fig. 4B, 3 hours, donor panel). Interestingly, also in lack-of-function mutant macrophages, FPN1 was recruited to the plasma membrane (Fig. 4B, p.G80S panel), although to a lesser extent than in donors, and normally internalized with Hepc (although in somewhat larger cytoplasmic vesicles than in donor macrophages).

We then explored the early steps of Hepc/FPN1 biology and FPN1 degradation. After exposure of macrophages

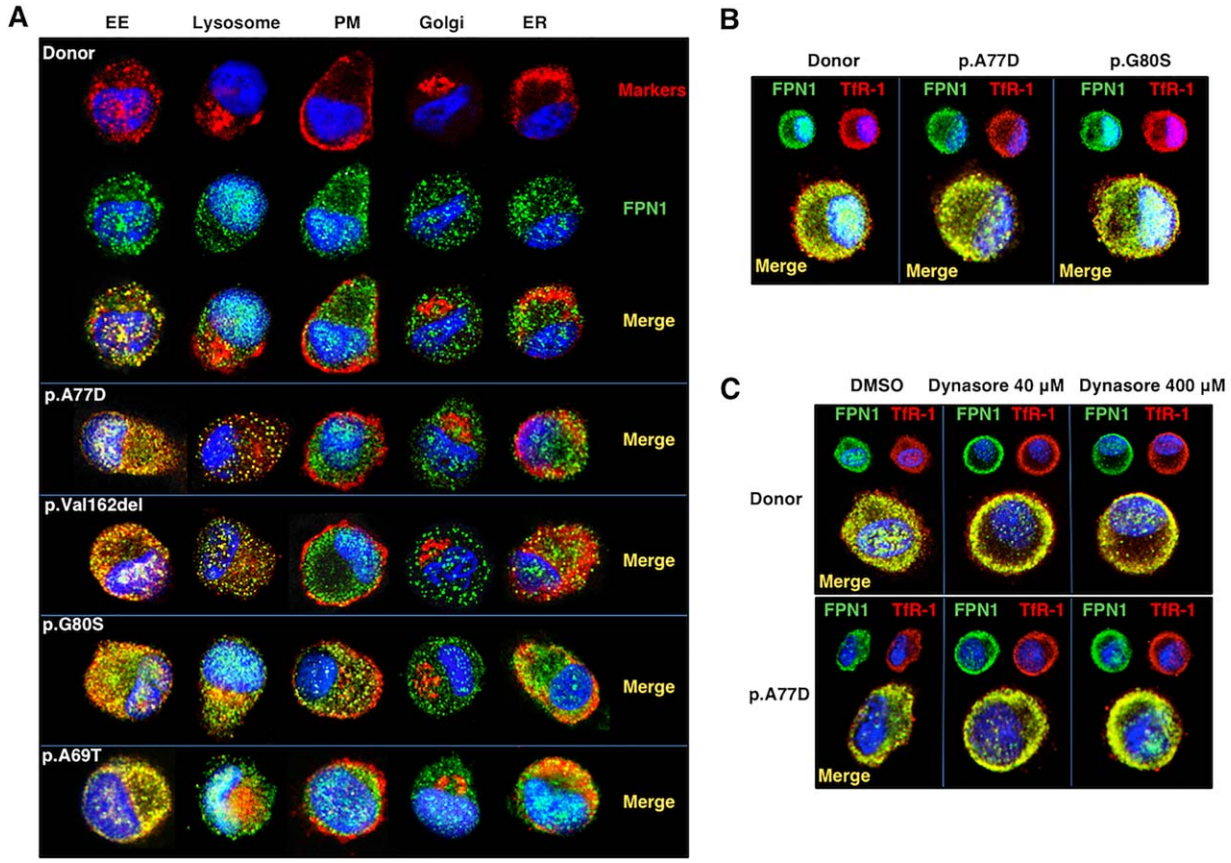

FIG. 3. WT and mutant FPN1 cycles in the early endosome/plasma membrane compartment in human macrophages. (A) Coimmunofluorescence staining of FPN1 (green) with markers (red) for early endosomes, EE (EEA-1), lysosomes (LAMP-1), plasma membrane, PM (Na,K-ATPase), Golgi (golgin-97), and endoplasmatic reticulum, ER (calnexin), shows that FPN1 colocalizes with early endosomes and lysosomes (merge panels, yellow) in p.A77D, p.G80S, and pVal162del macrophages, whereas it is almost exclusively localized in the EE compartment, in p.A69T and donor macrophages. (B) Coimmunostaining of FPN1 (green) with TfR1 (red; a marker for the early endocytic recycling compartment) shows that FPN1 colocalizes with TfR1 in donor as well as in p.G80S and p.A77D macrophages. (C) Treatment of macrophages from donors and p.A77D patients with dynasore to block dynamin-dependent endocytosis leads to accumulation of both FPN1 and TFR1 in the PM compartment.

to Hepc for 6 hours (Fig. 4C, Hepc panel), the 100- and ~55-kDa MW FPN1 form was no longer detectable, whereas a ~60-kDa MW FPN1 form (Fig. 4C, asterisk) appeared, both in normal and diseased macrophages (Fig. 4C, lanes 8 and 10 vs. lanes 2 and 4, respectively), but this was not the case with p.A69T "Hepc-resistant" macrophages (Fig. 4C, lanes 11 and 12).

DISTINCT PLASMA MEMBRANE EXPRESSION OF FPN1 IN PATIENT MACROPHAGES IN RESPONSE TO Hb-IRON

Hb-iron is a known stimulus for FPN1 expression and traffic to the plasma membrane.[41] We preliminary tested the response of human macrophages to different heme sources, namely, Hb and aged red blood cells. In both settings, we found a similar shift of FPN1 toward the plasma membrane (Fig. 5A). However, attributed to better control and reproducibility of the experimental procedures, we opted for the use of Hb in the following experiments in which macrophages were also incubated in the presence Dx, a known inducer of CD163 expression and Hb uptake.[35] In donor macrophages, Hb-Dx treatment led to a marked expression of FPN1 at the plasma membrane, as assessed by coimmunostaining with an antibody against Na,K-ATPase, a plasma membrane marker (Fig. 5B). However, in both p.G80S and p.A77D macrophages, Hb-Dx exposure was unable to recruit FPN1 to the plasma membrane, whereas it

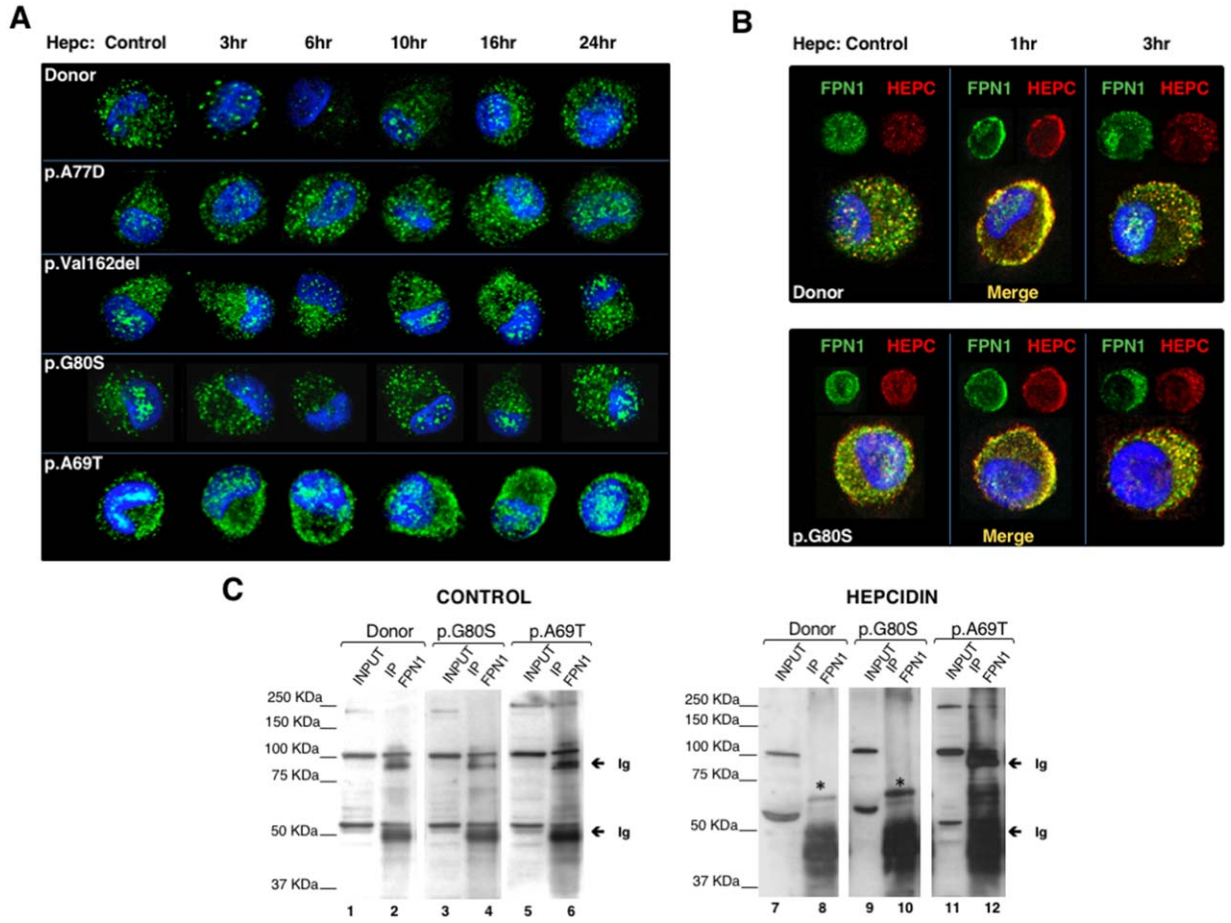

FIG. 4. Effect of Hepc on FPN1 expression and localization. (A) Immunofluorescence time-course analysis of FPN1 (green) in macrophages from healthy donors and p.A77D, p.Val162del, p.G80S, and p.A69T patients after incubation with Hepc. In donor macrophages, Hepc-induced FPN1 degradation starts at 3 hours and peaks at 6 hours, with full protein re-expression at 24 hours. As expected, in Hepc-resistant p.A69T mutant cells, FPN1 is not degraded after 3-6 hours of Hepc exposure. Yet, FD macrophages showed a persistent FPN1 staining at the same time points (see text for comments). (B) FPN1-Hepc colocalization studies by immunofluorescence show that both in donor and p.G80S macrophages, after 1 hour of hepcidin exposure, FPN1 (green) is recruited to the plasma membrane and colocalizes with Hepc (red), whereas after 3 hours both Hepc and FPN1 are internalized in cytoplasmic vesicles. (C) WB analysis of total protein extracts (INPUT) immunoprecipitated with an anti-FPN1 antibody from donor or diseased macrophages incubated for 6 hours in the absence (control panel) or presence of Hepc (Hepc panel). After exposure of macrophages to Hepc, an FPN1 form of around 62 kDa appears (stars in lanes 8 and 10). Arrows indicate specific signal for FPN1 and IgG. Abbreviations: Ig, immunoglobulin; IgG, immunoglobulin G.

dramatically increased cell membrane expression of FPN1 in p.A69T macrophages (Fig. 5B, merge panel). In agreement with previous experiments, when donor and p.A69T macrophages were exposed to Hb-Dx, both early endosomes and FPN1 readily shifted to the plasma membrane (Fig. 5C, merge panel), whereas, in p.G80S macrophages, whereas early endosome rapidly moved to the cell membrane, FPN1 largely remained in the cytoplasm (Fig. 5C, merge panel). Under these circumstances, intracellular ferritin content appreciably decreased in Hb-Dx-treated donor cells whereas it did not change in G80S macrophages and slightly increased in A77D macrophages (Fig. 5D), indicating intracellular iron retention in FD macrophages. Accordingly, iron efflux in the medium significantly increased in donor macrophages, but did not change in G80S and visibly decreased in A77D macrophages (Fig. 5E). Importantly, upon heme exposure, we did not detected higher MW forms of FPN (Fig. 5F), indicating that, even during strong induction of protein traffic to the cell surface, FPN1 does not multimerize and remains in the expected MW forms.

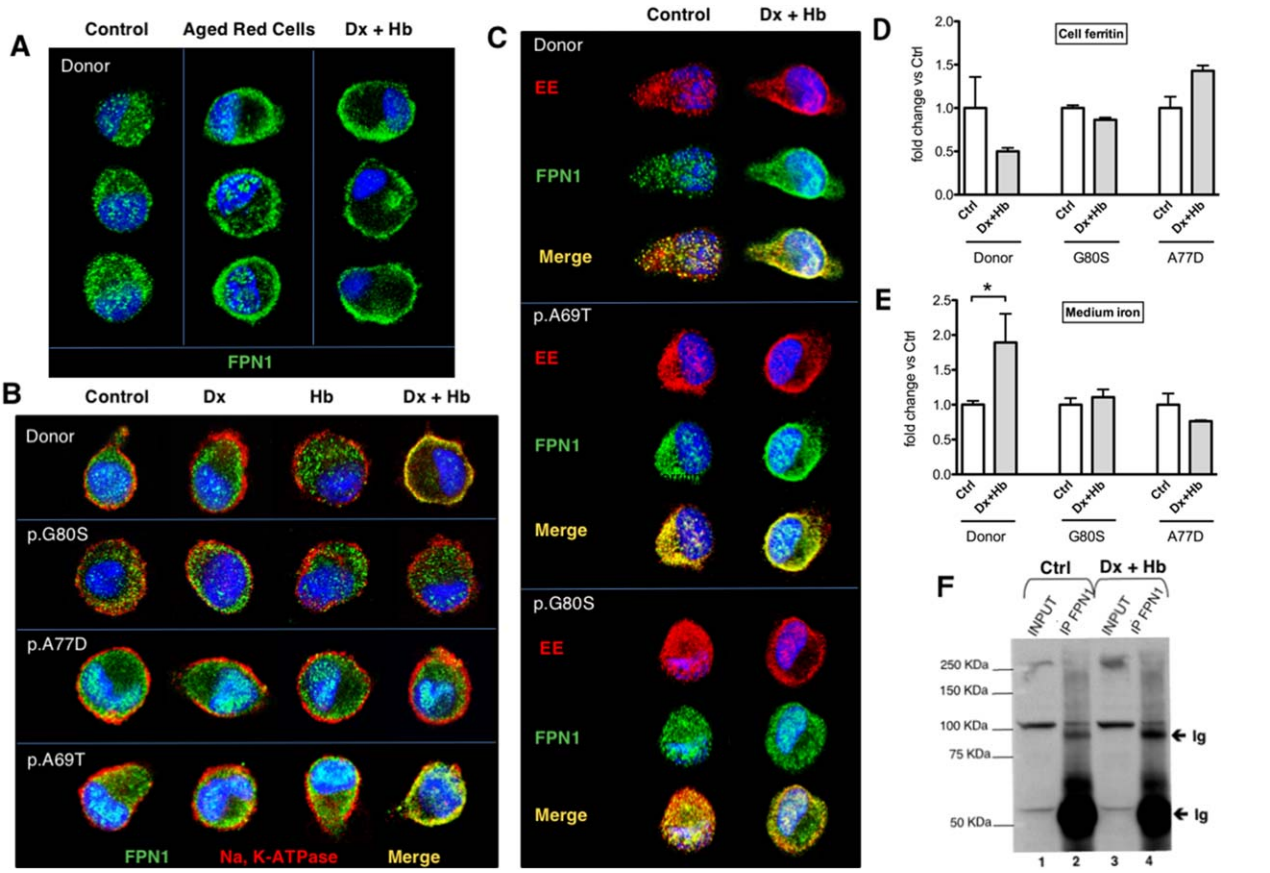

FIG. 5. Hb treatment leads to FPN1 membrane targeting in donor and Hepc-resistant FPN1—but not in lack-of-function FD macrophages, which fail to export iron. (A) Macrophages from healthy donors were incubated in the absence (Control) or presence of aged erythrocytes (Aged Red Cells), or of Dx+Hb. Coimmunofluorescence staining of FPN1 (green) and nucleus (blue) shows that both treatments mobilize the FPN1 to the periphery of the cell. (B) Macrophages from healthy donors and patients carrying mutant FPN1 (p.G80S, p.A77D, and p.A69T) were incubated in the absence (Control) or presence of Dx, Hb, or Dx+Hb (see Patients and Methods for details). Coimmunofluorescence staining of FPN1 (green) and Na,K-ATPase (red), a plasma membrane marker, merge (yellow). Only merge panels are shown. Dx-Hb treatment led to a prompt mobilization of FPN1 to the plasma membrane in donor and p.A69T macrophages, but not in FD macrophages. (C) Macrophages were treated as above. Using the EEA-1 early endosomes marker (red), in donor and p.A69T macrophages, both early endosomes and FPN1 are readily recruited to the plasma membrane upon Dx-Hb exposure, whereas in p.G80S macrophages, FPN1 largely remains in the cytoplasm. (D) Cell ferritin content in macrophages treated was assayed as reported in the Patients and Methods section. In donor macrophages, Hb-Dx treatment led to an appreciable decrease of intracellular ferritin, as compared to control cells, but this was not the case in G80S and A77D macrophages, indicating intracellular iron retention. Data are presented as fold change versus control cells, set to 1.0. The ferritin values are mean ± SEM of three different cell preparations from a representative patient as compared to cell preparations from a blood donor. $^*P < 0.05$. (E) Medium iron content in macrophages treated was assayed as reported in the Patients and Methods section. Medium iron significantly increased in donor macrophages exposed to Hb-Dx, but did not change in G80S and visibly decreased in A77D macrophages. Data are presented as fold change versus control cells, set to 1.0. The iron values are mean ± SEM of three different cell preparations from a representative patient as compared to cell preparations from a blood donor. $^*P < 0.05$. (F) WB analysis of the same amount of protein extracts (INPUT) from macrophages immunoprecipitated with anti FPN1 antibody (IP FPN1). Dx-Hb treatment did not modify the FPN1 WB pattern. Abbreviations: Ctrl, control; Ig, immunoglobulin.

Discussion

We found that in normal human macrophages, FPN1 is largely localized in the early endosomal cycling compartment within classic endocytic vesicle containing TfR1, whereas a marginal fraction is diverted to late endosomes and lysosomes for degradation. In human macrophages and HepG2 cells, we consistently detected two major bands at 100-kDa MW and ~55-kDa MW band by SDS-PAGE. These bands, however, most likely form during lysis, given that they are reduced by heating in the presence of

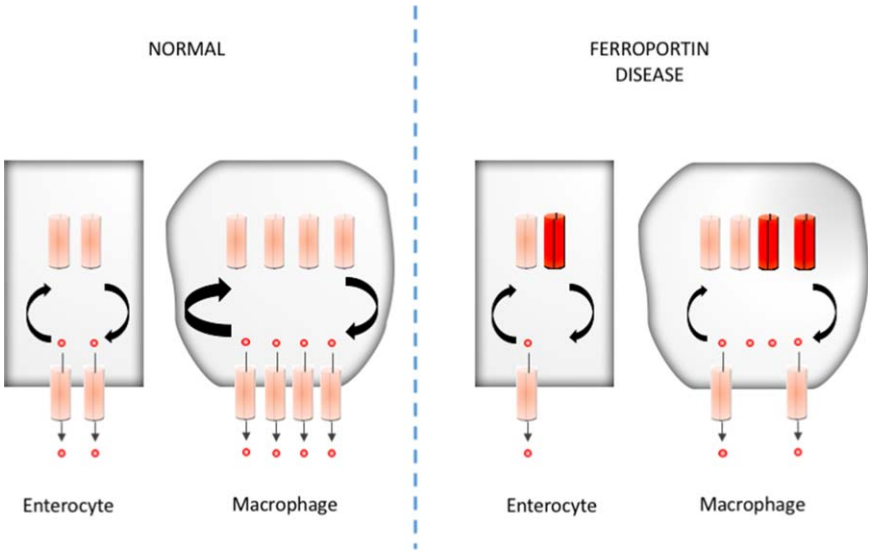

FIG. 6. Model of FD. Normal FPN1 traffics within the endosomal-cell membrane compartment as a monomer to export iron in cells with low iron turnover, such as enterocytes, and in larger quantity in cells with high iron turnover, such as tissue macrophages. In FD, FPN1 can still traffic to the cell membrane and export iron in enterocytes, but fails to do so in tissue macrophages requiring a larger amount of cell-surface–expressed FPN1.

IAA, leading to the appearance of the proper 65-kDa band. A similar FPN1 MW variability on WB analysis has been previously reported in liver, duodenum, and spleen of the same species by Canonne-Hergaux et al.[4] This may be attributed to different tissue- or species-specific posttranslational modifications of the protein, as well as to the fact that solubilization of highly hydrophobic proteins, especially multipass membrane proteins, is not efficient. In our hands, when protein extracts were subjected to enzymatic digestion with PGNaseF and EndoH, spleen FPN1 was promptly digested by PGNaseF (in agreement with Goncalves et al.[30]), but this was not the case for human macrophages and THP1 cells, whereas in HepG2 cells, both the 100-kDa MW and the ~55-kDa MW forms were partially digested. Yet, based on the human FPN1 expression experiments in MDCK cells, the peptide-competition experiments in human macrophages, the FPN1 siRNA experiments, and the response to Hepc inhibition, we can reasonably assume that the identified bands in human macrophages are electrophoretically different forms of FPN1. In order to define the native status of FPN1, we performed gel filtration of macrophage protein extracts. By size-exclusion chromatography, endosome-associated proteins form high-MW forms that are excluded, whereas solubilized native proteins can be partitioned and resolved. We conclude that native FPN1 in human macrophages is monomeric, in agreement with previous studies showing that FPN1 is a monomer *in vitro* and *in vivo*.[3,30-32]

After exposure of macrophages to Hepc, the physiological FPN1 inhibitor, FPN1 was recruited to the cell membrane, internalized, and progressively degraded. Under this circumstance, the ~62-kDa FPN1 form appeared. Finally, when normal macrophages were exposed to large amounts of Hb-iron, a physiological stimulus for FPN1 synthesis and traffic to the membrane, FPN1 rapidly shifted to the cell membrane (along with endosomal vesicles).

FPN1 biology in A69T macrophages was similar to that of normal macrophages under all experimental circumstances, except for the expected relative "resistance" to Hepc-induced degradation (Fig. 4C, lanes 11 and 12). These findings are in agreement with a previous *in vitro* study addressing p.A69T biology[12] and consistent with the patient's phenotype and the clinical diagnosis of FPN-associated hemochromatosis.[42]

A main objective of this study was to investigate FPN1 expression in human macrophages from FD patients carrying the p.A77D, p.G80S, and p.Val162del mutations and expressing the classic FD phenotype.[9,16,22,43-50] These FPN1 mutants have been previously investigated in cell lines, but with

controversial results in terms of cellular localization and iron transport capability.[3,5,6,20-22,46,49] In this study, we primarily aimed at verifying whether FPN1 reaches the cell membrane in FD macrophages. We found that FPN1 cycles in the early endosomal vesicles are detectable at the plasma membrane in FD macrophages and respond to Hepc as in donor macrophages. This does not support a "classic" dominant-negative model proposed by previous *in vitro* studies, where the mutant allele product is retained intracellularly and precludes traffic and membrane targeting of the WT allele product.[21,29] In general, in FD macrophages, a larger fraction of FPN1 resides in the late-endosome/lysosome compartment as compared to donor and A69T macrophages, thus suggesting a higher degradation rate of FPN1 (Fig. 3A). In Fig. 4A, the immunofluorescence signal in p.A77D, p.G80S, and p.Val162del mutations persists after 3-6 hours of Hepc exposure. We believe this pattern indicates that whereas FPN1 is normally targeted to the cell membrane and internalized upon Hepc exposure (Fig. 4B), in lack-of-function macrophages a larger fraction of FPN1 remains intracellularly, likely engaged/engulfed within the degradation compartment, thus giving rise to a more intense or persistent intracellular fluorescence signal. This is also suggested by the IP studies reported in Fig. 4C, where a larger proportion of "Hepc-internalized" FPN1 was detected in FD macrophages as compared to donor macrophages (asterisks in p.G80S vs. Donor, Fig. 4C). We cannot exclude that a different class of lack-of-function macrophages FPN1 may differ in cycling efficiency, iron export capacity, and/or Hepc sensitivity, based on intrinsic structural properties of FPN1 and chemical state of iron in the channel.[11,12] In fact, in p.G80S FPN1 macrophages, we consistently detected a lower faction of FPN1 committed to lysosomal degradation as compared to p.A77D and p.Val162del macrophages (Figs. 3A and 4A). However, when FD macrophages were exposed to a heme load, regardless of the mutation, FPN1 was unable to reach the plasma membrane and export iron (Fig. 5D,E). Under our experimental conditions, FPN1 expression did not increase upon heme exposure, as shown by the assessment of FPN1 protein expression (see Fig. 5F) and evaluation of FPN1 mRNA levels by RT-PCR (data not shown). It seems that under such conditions, when more FPN1 is needed at the cell surface, a faulty mechanism, likely at the level of the degradation/cycling pathway, prevents sufficient FPN1 from reaching the cell surface (Fig. 6).

In conclusion, based on the results of our *ex vivo* experiments, we postulate that in FD, FPN1 monomers can still reach the cell surface and export iron in cells that are exposed *in vivo* to a relatively low flux of iron, such as enterocytes (Fig. 6). However, in cells undergoing *in vivo* high iron turnover, such as tissue macrophages, a traffic jam in the degradation and/or endocytic cycling pathways prevents sufficient FPN1 from reaching the plasma membrane. In Fig. 6, for clarity, mutated FPN1 was not depicted at the cell surface. However, this aspect has not been addressed in the present article, and it cannot be excluded that, as suggested by some reports,[3,9,12,20] lack-of-function mutant FPN1 can also reach the cell surface.

The proposed model is compatible with a monomeric protein structure and is consistent with the clinical manifestations of FD patients in whom increased iron deposits in hepatic macrophages (i.e., Kupffer cells) are visible at young age,[15,16] transferrin saturation is fairly normal throughout the patient's life (indicating that mutant FPN1 activity is not limiting for intestinal iron transfer), but become critically low in young female at menarche or after aggressive phlebotomy,[15,16] when high iron demands for erythropoiesis likely impose increased FPN1 traffic/cycling within tissue macrophages.

REFERENCES

1) Drakesmith H, Nemeth E, Ganz T. Ironing out Ferroportin. Cell Metab 2015;22:777-787.
2) Nemeth E, Tuttle MS, Powelson J, Vaughn MB, Donovan A, Ward DM, et al. Hepcidin regulates cellular iron efflux by binding to ferroportin and inducing its internalization. Science 2004; 306:2090-2093.
3) Rice AE, Mendez MJ, Hokanson CA, Rees DC, Bjorkman PJ. Investigation of the biophysical and cell biological properties of ferroportin, a multipass integral membrane protein iron exporter. J Mol Biol 2009;386:717-732.
4) Canonne-Hergaux F, Donovan A, Delaby C, Wang HJ, Gros P. Comparative studies of duodenal and macrophage ferroportin proteins. Am J Physiol Gastrointest Liver Physiol 2006;290: G156-G163.
5) Schimanski LM, Drakesmith H, Merryweather-Clarke AT, Viprakasit V, Edwards JP, Sweetland E, et al. In vitro functional analysis of human ferroportin (FPN) and hemochromatosis-associated FPN mutations. Blood 2005;105:4096-4102.
6) Drakesmith H, Schimanski LM, Ormerod E, Merryweather-Clarke AT, Viprakasit V, Edwards JP, et al. Resistance to hepcidin is conferred by hemochromatosis-associated mutations of ferroportin. Blood 2005;106:1092-1097.
7) Liu XB, Yang F, Haile DJ. Functional consequences of ferroportin 1 mutations. Blood Cells Mol Dis 2005;35:33-46.

8) De Domenico I, Ward DM, Musci G, Kaplan J. Evidence for the multimeric structure of ferroportin. Blood 2007;109:2205-2209.
9) Wallace DF, Harris JM, Subramaniam VN. Functional analysis and theoretical modeling of ferroportin reveals clustering of mutations according to phenotype. Am J Physiol Cell Physiol 2010;298:C75-C84.
10) Le Gac G, Ka C, Joubrel R, Gourlaouen I, Lehn P, Mornon JP, et al. Structure-function analysis of the human ferroportin iron exporter (SLC40A1): effect of hemochromatosis type 4 disease mutations and identification of critical residues. Hum Mutat 2013;34:1371-1380.
11) Bonaccorsi di Patti MC, Polticelli F, Cece G, Cutone A, Felici F, Persichini T, Musci G. A structural model of human ferroportin and of its iron binding site. FEBS J 2014;281:2851-2860.
12) Praschberger R, Schranz M, Griffiths WJ, Baumgartner N, Hermann M, Lomas DJ, et al. Impact of D181V and A69T on the function of ferroportin as an iron export pump and hepcidin receptor. Biochim Biophys Acta 2014;1842:1406-1412.
13) Taniguchi R, Kato HE, Font J, Deshpande CN, Wada M, Ito K, et al. Outward- and inward-facing structures of a putative bacterial transition-metal transporter with homology to ferroportin. Nat Commun 2015;6:8545.
14) Pietrangelo A. The ferroportin disease. Blood Cells Mol Dis 2004;32:131-138.
15) Pietrangelo A, Montosi G, Totaro A, Garuti C, Conte D, Cassanelli S, et al. Hereditary hemochromatosis in adults without pathogenic mutations in the hemochromatosis gene [see comments]. N Engl J Med 1999;341:725-732.
16) Montosi G, Donovan A, Totaro A, Garuti C, Pignatti E, Cassanelli S, et al. Autosomal-dominant hemochromatosis is associated with a mutation in the ferroportin (SLC11A3) gene. J Clin Invest 2001;108:619-623.
17) Njajou OT, Vaessen N, Joosse M, Berghuis B, van Dongen JW, Breuning MH, et al. A mutation in SLC11A3 is associated with autosomal dominant hemochromatosis. Nat Genet 2001;28:213-214.
18) Wallace DF, Clark RM, Harley HA, Subramaniam VN. Autosomal dominant iron overload due to a novel mutation of ferroportin1 associated with parenchymal iron loading and cirrhosis. J Hepatol 2004;40:710-713.
19) Sham RL, Phatak PD, West C, Lee P, Andrews C, Beutler E. Autosomal dominant hereditary hemochromatosis associated with a novel ferroportin mutation and unique clinical features. Blood Cells Mol Dis 2005;34:157-161.
20) McGregor JA, Shayeghi M, Vulpe CD, Anderson GJ, Pietrangelo A, Simpson RJ, McKie AT. Impaired iron transport activity of ferroportin 1 in hereditary iron overload. J Membr Biol 2005;206:3-7.
21) De Domenico I, Ward DM, Nemeth E, Vaughn MB, Musci G, Ganz T, Kaplan J. The molecular basis of ferroportin-linked hemochromatosis. Proc Natl Acad Sci U S A 2005;102:8955-8960.
22) De Domenico I, McVey Ward D, Nemeth E, Ganz T, Corradini E, Ferrara F, et al. Molecular and clinical correlates in iron overload associated with mutations in ferroportin. Haematologica 2006;91:1092-1095.
23) De Domenico I, Ward DM, Langelier C, Vaughn MB, Nemeth E, Sundquist WI, et al. The molecular mechanism of hepcidin-mediated ferroportin down-regulation. Mol Biol Cell 2007;18:2569-2578.
24) Mayr R, Janecke AR, Schranz M, Griffiths WJ, Vogel W, Pietrangelo A, Zoller H. Ferroportin disease: a systematic meta-analysis of clinical and molecular findings. J Hepatol 2010;53:941-949.
25) Griffiths WJ, Mayr R, McFarlane I, Hermann M, Halsall DJ, Zoller H, Cox TM. Clinical presentation and molecular pathophysiology of autosomal dominant hemochromatosis caused by a novel ferroportin mutation. HEPATOLOGY 2010;51:788-795.
26) Mayr R, Griffiths WJ, Hermann M, McFarlane I, Halsall DJ, Finkenstedt A, et al. Identification of mutations in SLC40A1 that affect ferroportin function and phenotype of human ferroportin iron overload. Gastroenterology 2011;140:2056-2063, 2063.e1.
27) Pietrangelo A, Caleffi A, Corradini E. Non-HFE hepatic iron overload. Sem Liv Dis 2011;31:302-318.
28) Donovan A, Lima CA, Pinkus JL, Pinkus GS, Zon LI, Robine S, Andrews NC. The iron exporter ferroportin/Slc40a1 is essential for iron homeostasis. Cell Metab 2005;1:191-200.
29) Zohn IE, De Domenico I, Pollock A, Ward DM, Goodman JF, Liang X, et al. The flatiron mutation in mouse ferroportin acts as a dominant negative to cause ferroportin disease. Blood 2007;109:4174-4180.
30) Goncalves AS, Muzeau F, Blaybel R, Hetet G, Driss F, Delaby C, et al. Wild-type and mutant ferroportins do not form oligomers in transfected cells. Biochem J 2006;396:265-275.
31) Schimanski LM, Drakesmith H, Talbott C, Horne K, James JR, Davis SJ, et al. Ferroportin: lack of evidence for multimers. Blood Cells Mol Dis 2008;40:360-369.
32) Pignatti E, Mascheroni L, Sabelli M, Barelli S, Biffo S, Pietrangelo A. Ferroportin is a monomer in vivo in mice. Blood Cells Mol Dis 2006;36:26-32.
33) Montosi G, Paglia P, Garuti C, Guzman CA, Bastin JM, Colombo MP, Pietrangelo A. Wild-type HFE protein normalizes transferrin iron accumulation in macrophages from subjects with hereditary hemochromatosis. Blood 2000;96:1125-1129.
34) Kagan JC, Su T, Horng T, Chow A, Akira S, Medzhitov R. TRAM couples endocytosis of Toll-like receptor 4 to the induction of interferon-beta. Nat Immunol 2008;9:361-368.
35) Schaer DJ, Boretti FS, Schoedon G, Schaffner A. Induction of the CD163-dependent haemoglobin uptake by macrophages as a novel anti-inflammatory action of glucocorticoids. Br J Haematol 2002;119:239-243.
36) Delaby C, Pilard N, Goncalves AS, Beaumont C, Canonne-Hergaux F. Presence of the iron exporter ferroportin at the plasma membrane of macrophages is enhanced by iron loading and down-regulated by hepcidin. Blood 2005;106:3979-3984.
37) Park EK, Jung HS, Yang HI, Yoo MC, Kim C, Kim KS. Optimized THP-1 differentiation is required for the detection of responses to weak stimuli. Inflamm Res 2007;56:45-50.
38) Abboud S, Haile DJ. A novel mammalian iron-regulated protein involved in intracellular iron metabolism. J Biol Chem 2000;275:19906-19912.
39) Miluzio A, Beugnet A, Grosso S, Brina D, Mancino M, Campaner S, et al. Impairment of cytoplasmic eIF6 activity restricts lymphomagenesis and tumor progression without affecting normal growth. Cancer Cell 2011; 19:765-775.
40) Thomas TC, McNamee MG. Purification of membrane proteins. Guide to protein purification. In: Deutscher MF, ed. Methods in Enzymology Series 182. San Diego, CA: Academic; 1990:499-520.
41) Mahler HC, Friess W, Grauschopf U, Kiese S. Protein aggregation: pathways, induction factors and analysis. J Pharm Sci 2009;98:2909-2934.
42) Delaby C, Pilard N, Puy H, Canonne-Hergaux F. Sequential regulation of ferroportin expression after erythrophagocytosis in murine macrophages: early mRNA induction by haem, followed

by iron-dependent protein expression. Biochem J 2008;411:123-131.
43) Pietrangelo A. Hemochromatosis: 15 years since hepcidin. Gastroenterology 2015;149:1240-1251.
44) Wallace DF, Pedersen P, Dixon JL, Stephenson P, Searle JW, Powell LW, Subramaniam VN. Novel mutation in ferroportin1 is associated with autosomal dominant hemochromatosis. Blood 2002;100:692-694.
45) Zoller H, McFarlane I, Theurl I, Stadlmann S, Nemeth E, Oxley D, et al. Primary iron overload with inappropriate hepcidin expression in V162del ferroportin disease. HEPATOLOGY 2005;42:466-472.
46) Subramaniam VN, Wallace DF, Dixon JL, Fletcher LM, Crawford DH. Ferroportin disease due to the A77D mutation in Australia. Gut 2005;54:1048-1049.
47) Pietrangelo A, Corradini E, Ferrara F, Vegetti A, De Jong G, Luca Abbati G, et al. Magnetic resonance imaging to identify classic and nonclassic forms of ferroportin disease. Blood Cells Mol Dis 2006;37:192-196.
48) Lim FL, Dooley JS, Roques AW, Grellier L, Dhillon AP, Walker AP. Hepatic iron concentration, fibrosis and response to venesection associated with the A77D and V162del "loss of function" mutations in ferroportin disease. Blood Cells Mol Dis 2008;40:328-333.
49) McDonald CJ, Wallace DF, Ostini L, Bell SJ, Demediuk B, Subramaniam VN. G80S-linked ferroportin disease: classical ferroportin disease in an Asian family and reclassification of the mutant as iron transport defective. J Hepatol 2011;54:538-544.
50) Wolff F, Bailly B, Gulbis B, Cotton F. Monitoring of hepcidin levels in a patient with G80S-linked ferroportin disease undergoing iron depletion by phlebotomy. Clin Chim Acta 2014;430:20-21.

Supporting Information

Additional Supporting Information may be found at onlinelibrary.wiley.com/doi/10.1002/hep.29007/suppinfo.